Pergamon

Journal of Structural Geology, Vol. 17, No. 7, pp. 1025 to 1034, 1995

0191-8141/95 $9.50 + 0.00

0191-8141(94)00131-6

Fault slip evolution determined from crack-seal veins in pull-aparts and their implications for general slip models

IAN DAVISON

Department of Geology, Royal Holloway, University of London, Egham, Surrey, TW20 0EX, U.K.

(*Received* 7 *April* 1994; *accepted in revised form* 15 *November* 1994)

Abstract—Most observations of fault slip history are limited to a short period of a fault's lifetime (usually less than five major earthquake cycles) and are therefore not representative of long-term slip behaviour. A new approach to determine more complete slip histories on small inactive faults is outlined, where calcite-filled veins produced by individual slip events are measured. Two normal faults are described from the south Bristol Channel area, near Kilve, north Somerset, U.K. Fault 1 had a variable slip evolution, with variable slip magnitudes through time, but a smooth and fairly constant cumulative increase in displacement. Fault 2 also has a variable slip history but with temporary repetition of similar-sized (characteristic) slip events which were limited to a maximum of eight successive increments. Each set of temporary characteristic events was followed by a period of variable slip. On both faults there were no significant changes in slip increments immediately preceding or following the larger slip events. The average amount of cumulative slip per event at different localities was either constant, accelerated, or decelerated during the fault growth history. The two faults show a slip pattern where the total displacement along the fault varies smoothly, and magnitude of slip increment at any point is highly variable through time. The data from Fault 2 suggests that the central area, where displacement was a maximum, resulted from larger slip for each event rather than more frequent events of similar magnitude, whereas Fault 1 suggests more frequent slip events occurred in the centre of the fault to produce the displacement maximum.

INTRODUCTION

Determination of slip patterns on faults provides an important constraint on their growth behaviour. Observations of seismicity (usually less than five major earthquake cycles), surface rupture patterns, dating of associated events (e.g. tree death, marine terrace formation), have all been used to interpret the slip behaviour on large faults (e.g. Schwartz & Coppersmith 1984, Berryman & Beanland 1991). However, these data are usually limited to a much shorter period than the total active life of the fault. Several models of slip behaviour have been inferred from these short-term field studies and theoretical considerations which may be useful in prediction of recurrence time and magnitude of earthquakes (Shimazaki & Nakata 1980, Scholz 1989, Fig. 1):

(a) the *variable slip model* for normal and thrust faults in New Zealand (Berryman & Beanland 1991);
(b) the *uniform slip model* (Schwartz & Coppersmith 1984);
(c) the *characteristic earthquake model* which has been applied to strike-slip and normal faults in the western U.S.A. (Schwartz & Coppersmith 1984), and strike-slip faults in New Zealand (Berryman & Beanland 1991).

The characteristic earthquake model seems to hold for the short periods which are usually examined (usually less than 10,000 years, e.g. Schwartz & Coppersmith 1984). However, rupture lengths and slip magnitudes must eventually change through time, and barriers will be created and destroyed during fault growth (e.g. Scholz 1990). Thus, it is predicted that characteristic earthquakes may repeat for a certain number of cycles and then change with time to a new magnitude and slip distribution. This suggests another category of slip behaviour which has a variable slip behaviour with temporary characteristic earthquakes (Fig. 1d). Unfortunately, the various slip models are not easily testable using long-term slip evidence in the field.

This study tests the validity of such models on small faults by using a new approach to the examination of slip histories preserved as calcite-filled crack-seal veins (Ramsay 1980) in dilational pull-apart zones along faults (Fig. 2). However, previous models have been based on large faults and have used different fault attributes or seismicity measurements, whereas this study looks at two much smaller faults. It is still not known whether small faults have significantly different slip behaviour than large faults. Fracture toughness may be important in controlling the size of the crack-seal veins on the small scale, but large faults probably have other dominant controlling factors such as strain softening, fault interaction and linkage and large scale barriers. Further work is required to investigate these differences.

Each cracking event was produced by slip on the fault followed by a period of stability when fractures were re-cemented with calcite, this can be described as a type of stick-slip behaviour. The magnitude of slip increments can be obtained by measuring the vein extension parallel to the fault slip direction (Fig. 2). Magnitude of slip events is probably controlled by the strength of the rock, and because the rocks are affected by mineralization during faulting it is possible that fracture toughness may have changed during the evolution of the fault. The width of the fractures may not accurately represent the true amount of slip that occurred on the fault as the

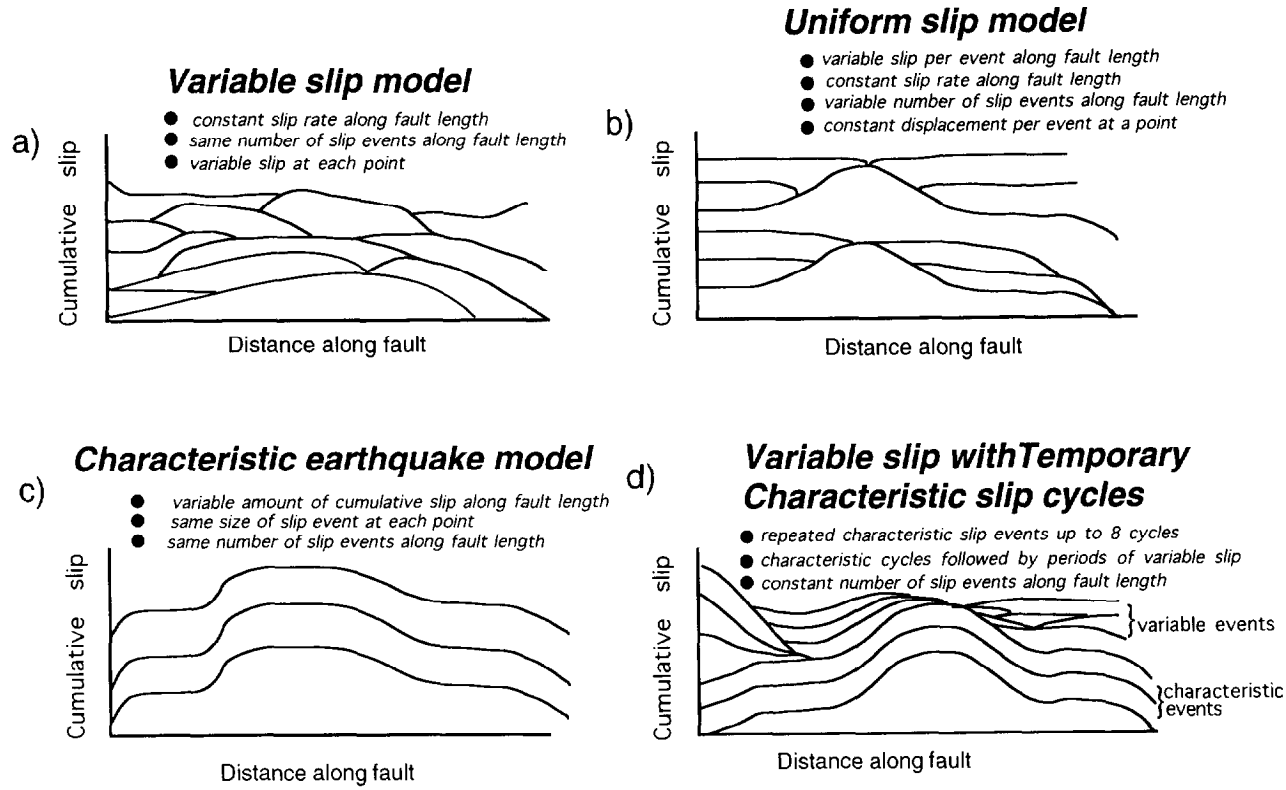

Fig. 1. Models of fault slip behaviour (a)–(c) after Schwartz & Coppersmith (1984). (d) The temporary characteristic earthquake model (this study on smaller faults).

availability of mineralizing fluid and crystallization velocity would also be important. There are no significant progressive changes in the width of the crack-seal veins produced, however, suggesting that mineralizing conditions and rheology remained fairly constant during the fault evolution.

When fault slip occurred, the hangingwall rock was broken near to the interface with the previous calcite vein fill (Fig. 2). The wall rock broke, rather than the contact between the vein and wallrock, because calcite cementation occurred over a limited distance (<1 mm) in the wallrocks after each slip episode. Breakage usually occurred along the edge of this cemented zone.

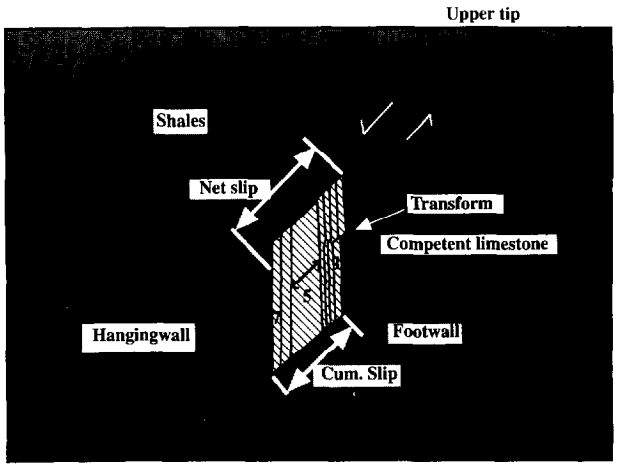

Fig. 2. Schematic development of crack-seal veins in dilational pull-apart zone along a normal fault. The sequence of pull-apart increments is numbered in the order produced by progressive breakage in the hangingwall of the fault zone.

Similar crack-seal textures have been recorded from faults and veins in limestone and mudstone from other areas; thrust faults in the Italian Apennines (Labaume *et al.* 1991) and the Makran accretionary wedge, Pakistan (Platt *et al.* 1988), strike-slip faults in the Arc Basin, south France (Gaviglio 1986) and veins in the Kodiak accretionary prism (Fisher & Brantley 1992). There is no control on the time-scale of deformation, although Main *et al.* (1994) have recently shown how quartz-filled crack-seal veins in Westerly granite can form within 100 h.

TECTONIC SETTING OF THE BRISTOL CHANNEL FAULTS

The two studied faults, and many similar occurrences, crop-out on the southern margin of the Bristol Channel Basin near Kilve, U.K. (Map Sheet Ordnance Survey ST 04/14, grid reference 1444 4444). The faults cut through organic-rich shales and argillaceous limestone of Early Jurassic age (Whittaker & Green 1983). Pull-aparts were created by refraction of the fault plane to steeper angles through the more competent limestone layers (Peacock & Sanderson 1992). Striations indicate that both faults are dip-slip normal faults. Vitrinite reflectance data from adjacent areas indicate that the sediments were buried to at least 1.5 km, and possibly as much as 3 km, during basin formation, which places a maximum limit on the faulting depth (Cornford 1986). Oxygen and carbon isotope data (Hayward 1991, and Appendix of this paper) on the calcite veins suggest that

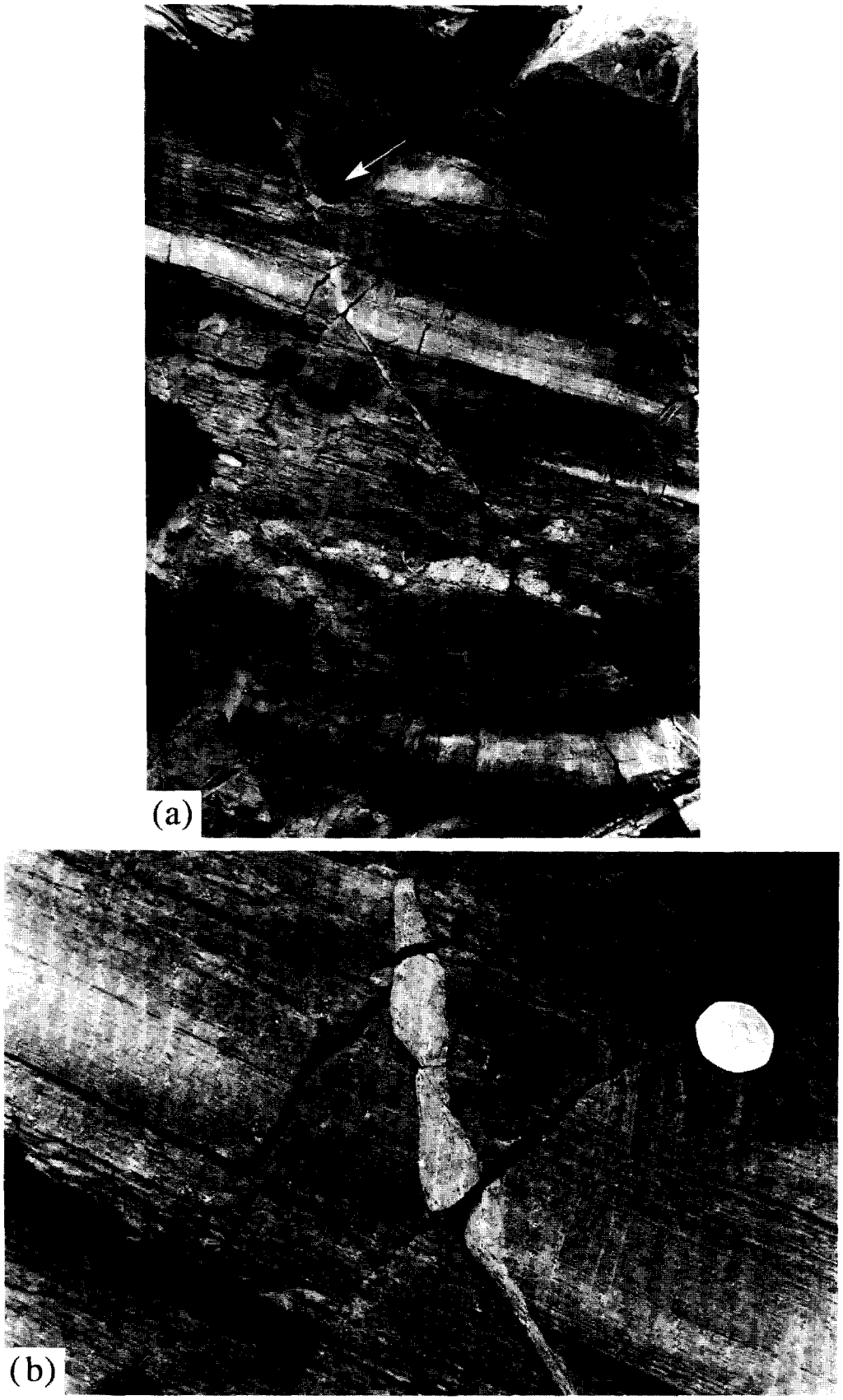

Fig. 3. (a) Fault 1 showing well-developed pull-aparts where the fault refracts to a steeper angle through more competent beds. Lens cap (arrowed) is 4.5 cm wide. (b) Close-up of pull-apart in the middle of the fault at location 4. Coin is 3 cm in diameter.

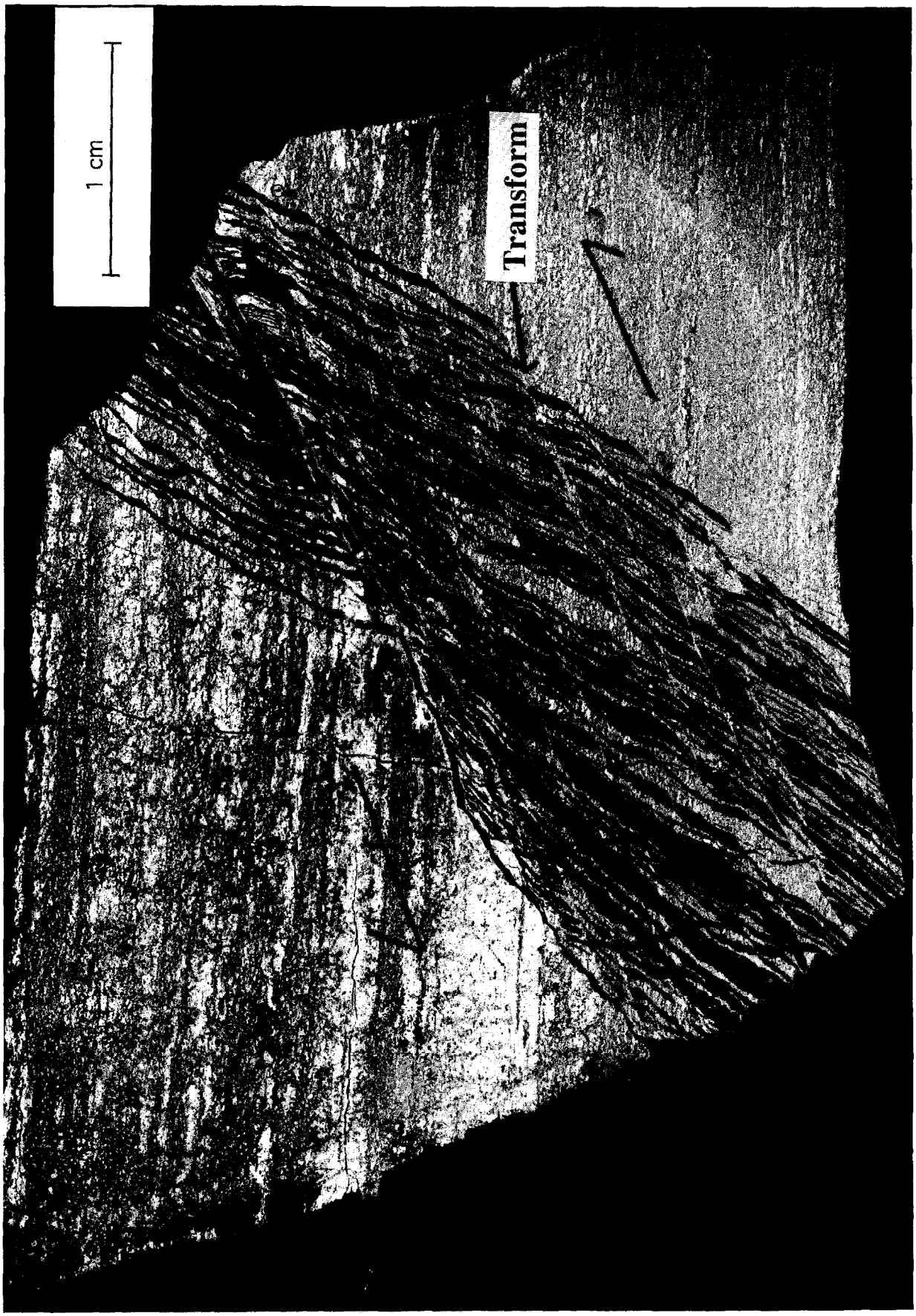

Fig. 4. Negative print of thin section through the fault zone 1 at location 4 [shown on Fig. 3(b)]. Darkest grey strips are stained calcite, and the lighter grey strips are wallrock shales. Sedimentary bedding in the surrounding calcareous shales is sub-horizontal.

the mineralizing fluids were hotter than the surrounding rocks. The calcite composition of the wallrock shales and limestones is less ferroan than the crack-seal vein infill.

VEIN TEXTURES

Both faults have similar vein-fill textures which consist of equant to slightly elongate ferroan-calcite grains which grow approximately perpendicular to the vein walls. The calcite grain size is fairly constant and varies from one half to the full width of the vein increments. Cathodoluminscence studies do not show any zoning of the calcite in each individual vein fill, nor is there any progressive change in luminescence across the whole pull-apart zone. There is a distinct difference in the luminescence of the vein-fill calcite and the host rock calcite, which has a brighter luminescence. Stable isotope data from the individual veins indicate there is little change in fluid composition between the slip events. These observations suggest that all the pull-apart veins formed during the same tectonic episode and each slip event produced a void which was filled by deposition from a mineralizing fluid with a homogenous composition. The thin veins which are almost vertical in Fig. 4 cut across the earlier pull-apart veins, and are distinctly more luminescent. These may have formed during later inversion which affected this area in Cretaceous to Tertiary times.

SLIP EVOLUTION OF FAULT 1

This fault is situated at the first faulted sea cliff face encountered approximately 100 m east of the Kilve stream. It is an antithetic fault to a larger northward dipping fault (Fig. 3a). It has a maximum displacement of 4 cm which dies out upwards and downwards over a length of 1.1 m in vertical outcrop profile (Figs. 3a & b). However, the upper fault tip was not observed as the fault displacement is transferred onto a bedding-planar fault.

Where the wall rock broke along an irregular surface, the sequence of slip events can be determined (Figs. 2 and 4). The irregularities in the fault plane initiate offsets in the vein fill analogous to transform faults, which are parallel to the main fault plane and have an apparent sense of offset opposite to the movement sense on the main fault (Figs. 2 and 4). The offsets are largest at the footwall contact and progressively decrease to zero towards the hangingwall (Fig. 4). This indicates that the faults progressively broke near the hangingwall contact (Fig. 2). Width of the veins (slip increments) measured parallel to the slip vector (main fault plane) is fairly constant along their length, hence, measurements can be made at any point across the pull-apart. Measurements were taken on thin sections through the pull-aparts which were printed directly from an enlarger onto photographic paper. The prints were enlarged up to 16 times to enable measurements to be made to an accuracy of $\pm 20\,\mu$m.

The width of the wall rock slivers plucked from the vein walls varies quite markedly from several microns to several centimetres and does not appear to be related to the size of the immediately preceding or following slip increment (Fig. 4). Not all of the displacement is recorded as crack-seal veins. The fault displacement at localities 3 and 4 on Fig. 5 was 40 mm, and the total vein width of the crack-seal veins is 22 mm. The remaining 18 mm of displacement is probably taken up by pressure solution, volume change and plastic deformation without development of tension cracks. It is difficult to measure how this strain is distributed between the vein and the wall-rock slivers (Fig. 4). Ductile deformation of the wall rocks and pre-existing vein calcite may have allowed veins to collapse inwards from a larger void. Hence, the exact slip magnitudes of each event may not be faithfully recorded by the present-day vein width. However, the recognition of slip patterns and relative slip magnitudes is the main aim of this study, and many more consecutive slip increments are recorded by crack-seal veins than any other known method of slip determination thus making this a valuable alternative approach.

The number of recorded slip increments varies from 39 at locality 1 up to 81 at locality 6 (Table 1 and Fig. 6). Slip increments vary from a minimum of 29 μm at locality 3 to a maximum of 2229 μm at locality 4 (Fig. 6). The lower parts of the fault (locations 5 and 6) have smaller slip increments and more constant rates of slip increase per event (Fig. 6). It is difficult to explain this variation, but it may be due to these locations having smaller irregularities which produced smaller pull-aparts compared to the other localities (1–4).

The larger slip increments at each locality occurs in the middle to latter half of the fault growth sequence. There is no distinct change in slip increments immediately preceding or following the larger events (Table 1). Semi-variogram statistical analysis has been performed on the slip sequences and this indicated a random pattern of slip events. There is a marked tendency for the larger slip events to cluster, but they are separated by up to six smaller events (Fig. 6 and Table 1). There are usually one or more slip magnitudes which are most frequent at each locality. These vary between 120 and 600 μm, and lie at the lower end of the slip magnitude range (Fig. 6b). The rate of cumulative slip increase per event remained fairly constant at localities 5 and 6, but accelerated or decelerated over ten or more events at localities 1–4. Several larger increments of slip can be correlated between locations 1 and 4 (arrowed in Fig. 6a). The slip data have been analysed to identify characteristic repeated cycles of three or more successive slip events with magnitudes which do not vary by more than 20% of the first slip event in the sequence. There is no definition of a characteristic earthquake slip sequence, and the 20% value used here was arbitrarily chosen. Only five such characteristic sequences with three successive events were identified (Table 1), which suggests that neither the characteristic nor the temporary

Table 1. List of fault slip increments in their estimated order of occurrence at the six locations on Fault 1. Slip in microns. Bold italicized numbers refer to slip cycles where three or more successive slip events have magnitudes which do not vary by more than 20% from the first slip event in the cycle

Event No.	Loc. 1	Loc. 2	Loc. 3	Loc. 4	Loc. 5	Loc. 6	Loc. 6 cont.	Loc. 6 cont.
1	258	605	117	534	357	88	61	***259***
2	386	499	527	534	220	118	62	***265***
3	193	107	644	168	266	59	63	***294***
4	837	694	351	336	426	765	64	88
5	477	71	293	382	456	235	65	294
6	580	106	328	191	266	147	66	294
7	451	356	117	550	175	706	67	494
8	902	178	59	92	486	382	68	1000
9	206	71	29	458	152	235	69	88
10	322	43	58	76	266	235	70	588
11	773	178	234	840	190	471	71	412
12	644	36	29	168	***304***	412	72	88
13	231	299	737	114	***350***	588	73	29
14	335	107	23	76	***350***	471	74	88
15	418	71	87	61	171	853	75	176
16	32	747	843	46	190	88	76	588
17	463	36	29	153	210	176	77	411
18	258	71	351	1069	350	176	72	88
19	580	71	556	382	198	318	73	29
20	284	997	316	76	380	118	74	88
21	387	284	234	763	593	176	75	176
22	387	570	468	229	160	88	76	147
23	129	321	146	458	160	147	77	588
24	232	356	796	473	274	306	78	235
25	1933	142	456	458	285	1029	79	235
26	232	285	410	153	836	500	80	59
27	580	107	1230	954	517	176	81	118
28	290	712	409	458	152	294		
29	258	855	526	427	76	176		
30	1804	214	410	305	53	71		
31	515	499	175	115	99	118		
32	838	641	1991	702	***114***	176		
33	1997	463	293	382	***137***	365		
34	206	285	422	496	***114***	88		
35	902	1887	2143	382	236	412		
36	192	303	878	153	84	176		
37	193	534	281	1542	99	618		
38	515	356	1663	534	722	118		
39	1353	356	176	550	152	176		
40		1780	176	2229	***228***	118		
41		783	234	229	***190***	353		
42		107	585	534	***236***	941		
43			205	1756	114	794		
44			410	***153***	152	1059		
45			556	***153***	152	541		
46			304	***153***	76	147		
47			176	534	114	88		
48			468	153	342	205		
49			375	420	399	412		
50			47	153	152	176		
51			351	229	646	176		
52				534	198	471		
53					152	88		
54					175	118		
55					273	***147***		
56					160	***147***		
57					108	***153***		
58					433	412		
59						206		
60						118		

Table 2. List of fault slip increments in their estimated order of occurrence at the five locations on Fault 2. Bold italicized numbers explained in caption to Table 1

Event No.	Loc. 7	Loc. 8	Loc. 9	Loc. 10	Loc. 11
1	***545***	550	835	82	114
2	***589***	326	835	164	230
3	***589***	584	1252	410	57
4	***635***	172	***501***	32.8	344
5	***601***	378	***501***	98	258
6	434	241	***501***	164	252
7	387	275	668	287	172
8	471	378	584	328	344
9	409	378	250	***656***	401
10	***310***	275	417	***656***	430
11	***310***	275	417	***656***	287
12	***279***	241	334	***656***	401
13	***263***	481	***501***	***492***	344
14	434	289	***584***	***492***	746
15	310	344	***501***	***574***	574
16	***295***	***247***	668	***492***	516
17	***260***	***254***	501	42	717
18	***279***	***220***	***751***	410	401
19	***291***	399	***751***	492	941
20	***325***	481	***668***	525	717
21	***279***	357	584	287	688
22	465	275	***501***	287	631
23	434	***344***	***501***	410	459
24	***372***	***378***	***501***	328	711
25	***372***	***344***	417	—	660
26	***372***	***378***	—	410	172
27	***357***	275	668	574	631
28	186	361	334	574	459
29	186	275	417	656	287
30	***217***	448	584	492	688
31	***217***	275	501	574	516
32	***217***	241	417	492	574
33	***204***	206	33	328	746
34	***267***	275	334	328	631
35	***248***	344	33	492	631
36	***248***	309	334	442	459
37	***279***	247	***668***	656	482
38	93	137	***668***	574	642
39	186	292	***668***	410	631
40	161	192	***501***	82	487
41	217	378	***501***	1148	631
42	***248***	392	***501***	—	516
43	***279***	309	167	***574***	482
44	***279***	384	167	***492***	401
45	***235***	344	250	***492***	367
46	***248***	309	501	***492***	459
47	310	240	334	246	516
48	310	240	501	492	344
49	391	357	334	246	321
50	279	240	501	246	***401***
51	217	343	417	656	***430***
52	248	103	417	656	***367***
53	186	34	250	164	***401***
54	***217***	51	417	328	597
55	***217***	137	501	246	287
56	***217***				516
57					688
58					436
59					***551***
60					***516***
61					***574***
62					***487***
63					660

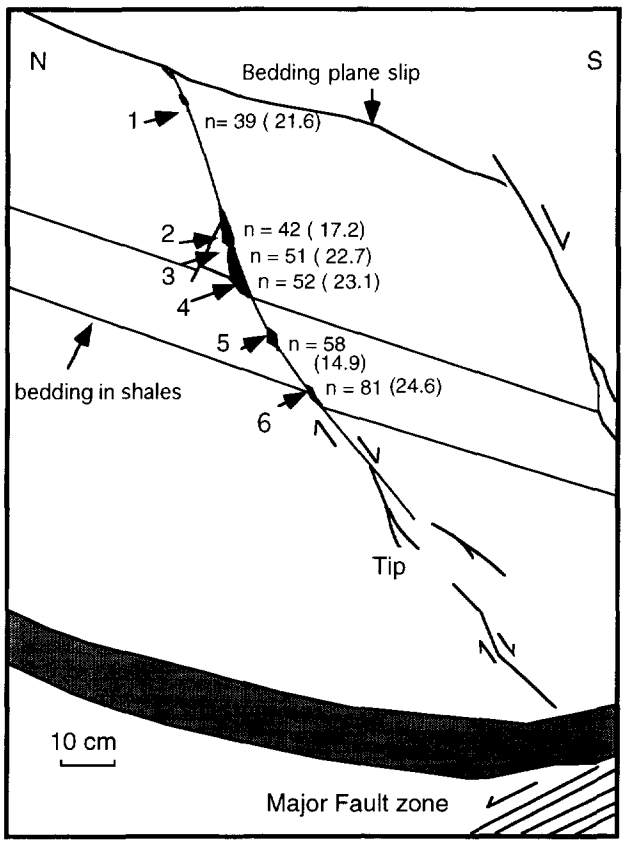

Fig. 5. Outcrop sketch of Fault 1 cross-section showing measurement locations at pull-aparts (1–6), and details of slip histories. The black areas represent calcite veining in dilatational pull-apart zones. n = number of slip events recorded. Number in brackets is the total cumulative slip in mm recorded by the crack-seal veins.

characteristic slip models are applicable to this fault. Constant increase in cumulative slip per event also contradicts fault slip models which invoke a progressive increase in slip magnitude through time (e.g. Watterson 1986, Marrett & Allmendinger 1991). However, it must be remembered that such models were based on much larger faults and sampling of different fault attributes.

SLIP EVOLUTION OF FAULT 2

This fault is a N-dipping fault 20 m along strike and east of Fault 1. The fault links directly to a larger S-dipping fault, but dies out upwards with a bifurcating tip (Fig. 7). Six samples have been examined from this fault, but only five of the samples gave a detailed slip evolution as one sample contained fibres and did not exhibit wall rock slivers, so that individual increments could not be measured. The cumulative fault slip and frequency plots of fault slip increments are shown in Fig. 8. Again only about 30% of the total fault slip is recorded by the pull-aparts, with the rest of the deformation probably distributed between pressure solution slip and plastic deformation of the calcite veins and wallrocks in the pull-aparts. The cumulative slip per event increased at a fairly constant rate at all five locations along the fault (Fig. 8). Large jumps in the cumulative slip are present at locations 9 and 10, but these are probably due to the fault breaking at the vein-wallrock contact for several slip increments so that the individual slip increments were not measurable. This has produced a fibrous growth of calcite across the largest veins. There is a marked most frequent slip increment at locations 9 and 10, two frequent slip increments at location 8 and a broader spread of slip increments at locations 7 and 11. The most frequent slip increments are in the middle to upper half of the slip increment size range, which is a different behaviour compared to Fault 1. There is a marked increase in the number of temporary characteristic earthquake cycles on this fault with 18 sequences of three or more slip events, and up to eight successive events in each cycle (Table 2). These temporary characteristic cycles are evenly distributed at each location along the fault and occur throughout the slip history (Table 2). Slip increments which are most frequent are all approximately 500 μm in magnitude at locations 9 and 11. There is a fairly constant distribution of slip increments along the fault from location 7 nearer the tip of the fault (58 events) compared to location 11 which registered 63 events.

CONCLUSIONS

A variety in fault slip behaviour has been demonstrated using this new approach to measuring small fault displacements. The number of slip increments decreases towards the fault tip on Fault 1 suggesting that maximum displacements build up on this fault was due to an increased number of slip events, and not due to an increase in the size of the slip increments at the centre of the fault. Whereas Fault 2 exhibits a behaviour where the number of slip increments remains constant along the fault, suggesting that rupture occurred over the whole length of the fault during each slip event with displacement decreasing towards the fault tip. Slip increments on the two faults do not support long-term characteristic earthquake behaviour, where constant-sized earthquakes occur at the same point on the fault. Characteristic earthquakes temporarily exist for up to eight successive events on Fault 2, but they are rare on Fault 1. This suggests that barriers were temporarily encountered on Fault 2, and the slip is characteristic for several cycles before a barrier breaks down and a new slip regime is imposed. This highlights the danger of using short-term slip measurements on active faults to infer long-term behaviour. The data from both faults are consistent with a variable slip model with occasional temporary characteristic slip cycles. Highly variable slip increments allow a smooth displacement variation to build-up along both faults.

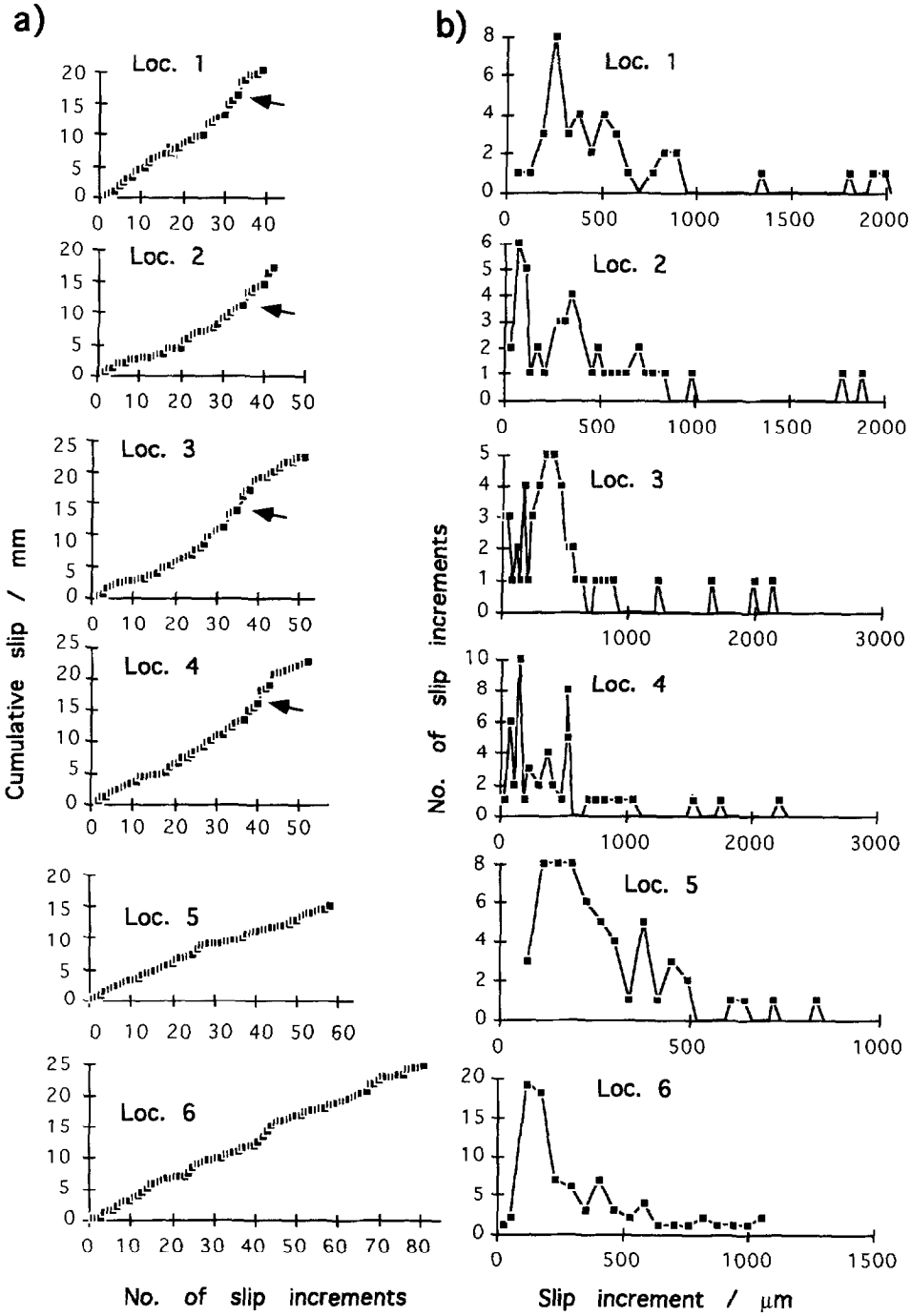

Fig. 6. Slip histories at six localities along the fault plane no. 1 shown in Fig. 5. (a) Cumulative displacement histories. (b) Slip frequency distribution.

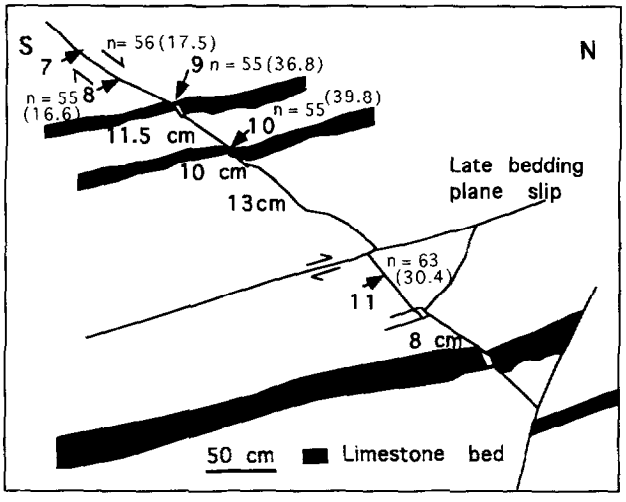

Fig. 7. Line drawing of Fault 2 showing the five pull-apart locations where displacement histories were measured. n = number of slip events recorded. Length values (in cm) are slip measured at the pull-aparts from bed offset.

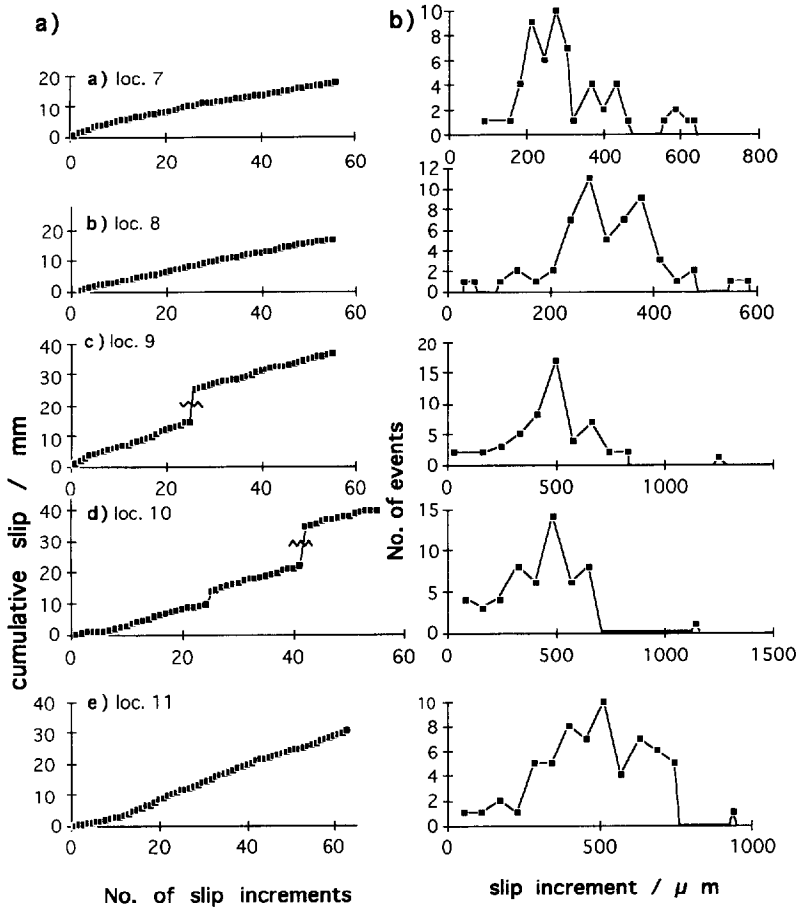

Fig. 8. (a) Cumulative displacement histories of five locations along Fault 2 shown in Fig. 7. (b) Slip frequency distribution of the five locations along Fault 2.

Acknowledgements—David Anastasio and an anonymous *JSG* reviewer are thanked for their very helpful reviews. David Mattey and Elizabeth Whittaker are thanked for providing the stable isotope analyses.

REFERENCES

Berryman, K. & Beanland, S. 1991. Variation in fault behaviour in different tectonic provinces of New Zealand. *J. Struct Geol.* **13**, 177–189.

Cornford, C. 1986. The Bristol Channel Graben: organic geochemical limits on subsidence and speculation on the origin of inversion. *Proc. Ussher Soc.* **6**, 360–367.

Fisher, D. M. & Brantley, S. L. 1992. Model overgrowth and vein formation: deformation and episodic fluid flow in an ancient subduction zone. *J. geophys. Res.* **97**, 20,043–20,061.

Gaviglio, P. 1986. Crack-seal mechanism in a limestone: a factor of deformation in strike-slip faulting. *Tectonophysics* **131**, 247–255.

Hayward, R. 1991. Mineralisation in fault zones, Watchet, N. Somerset. Unpublished M.Sc. thesis, Royal Holloway, University of London.

Labaume, P., Berty, C. & Laurent, Ph. 1991. Syn-diagenetic evolution of shear structures in superficial nappes: an example from the Northern Apennines (NW Italy). *J. Struct. Geol.* **13**, 385–398.

Main, I., Hutcheon, R., Meredith, P., Crawford, B. & Smart, B. 1994. Characteristic size effects during self-sealing brittle deformation. *Fault populations meeting 19–20 October 1994, Roy. Soc. Edin.* (extended abstract) 75–78.

Marrett, R. & Allmendinger, R. W. 1991. Estimates of strain due to brittle faulting: sampling of fault populations. *J. Struct. Geol.* **13**, 735–738.

Peacock, D. C. P. & Sanderson, D. J. 1992. Effects of layering and anisotropy on fault geometry. *J. geol. Soc. Lond.* **149**, 793–802.

Platt, J. P., Leggett, J. K. & Alam, S. 1988. Slip vectors and fault mechanics in the Makran accretionary wedge, south-west Pakistan *J. geophys. Res.* **93**, 7955–7973.

Ramsay, J. G. 1980. The crack-seal mechanism of rock deformation. *Nature* **284**, 135–139.

Scholz, C. H. 1989. Comments on models of earthquake recurrence. In: *Proceedings of Conference XLV-Fault Segmentation and Controls of Rupture Initiation and Termination* (edited by Schwartz, D. P. & Sibson, R. H.). *U.S. geol. Surv. Open-file Rep.* **89-315**, 350–360.

Scholz, C. H. 1990. *The Mechanics of Earthquakes and Faulting.* Cambridge University Press, Cambridge, U.K.

Schwartz, D. P. & Coppersmith, K. J. 1984. Fault behaviour and characteristic earthquakes: examples from the Wasatch and San Andreas Fault Zones. *J. geophys. Res.* **89**, 5681–5698.

Shimazaki, K. & Nakata, T. 1980. Time-predictable recurrence model for large earthquakes. *Geophys. Res. Lett.* **7**, 279–282.

Tucker, M. E. & Wright, V. P. 1990. *Carbonate Sedimentology.* Blackwell, Oxford, U.K.

Watterson, J. 1986. Fault dimensions, displacements and growth. *Pure & Appl. Geophys.* **124**, 365–373.

Whittaker, A. & Green, G. W. 1983. Geology of the country around Weston-super-Mare, memoir for 1:50,000 geological sheet 279 new series, with parts of sheets 263 and 295. Geological Survey of Great Britain, Institute of Geological Sciences, Her Majesty's Stationery Office. p. 147.

APPENDIX

Stable isotope variation during faulting

The carbon and oxygen isotope variation has been investigated across the veins in one of the fault zones to determine the conditions of mineralization and whether the faulting occurred during one tectonic episode. The analyses suggest that the mineralizing fluids which precipitated the calcite were not in equilibrium with the wall rock calcite. Oxygen isotope composition in the wall rocks ranges from −7.39 to −6.65 and $\partial^{13}C_{PDB}$ ranges from 0.52 to 0.70, whereas the

vein calcite all has a similar composition of $\partial C^{13}{}_{PDB}$ around 0.1 and $\partial^{18}O_{SMOW}$ ranges between −10.4 and −9.7 (Fig. A1), similar values were also found by Hayward (1991). The carbon and oxygen isotope composition of the carbonate across the fault remain constant indicating that all increments of slip were accompanied by approximately the same type of mineralizing fluid and all the fault increments probably occurred at approximately the same depth of burial (Fig. A1). An indication of the isotopic composition of the water from which the calcite precipitated can be derived from using the equilibrium relationship described in Tucker & Wright (1990, p. 310). Assuming a mineralizing temperature of 60°C as suggested by the vitrinite reflectance values (Cornford 1986), the $\partial^{18}O_{SMOW}$ values of −10 in the veins suggests a meteoric origin for the waters with a $\partial^{18}O_{SMOW}$ composition of approximately −20.

Table A1. Stable isotope analytical results from location 9 on Fault 2. Locations of analyses are shown in Fig. A1. Estimated errors on these measurements are ± 0.1‰

Spec. No.	$\partial^{S13}C_{PDB}$	$\partial^{18}O_{SMOW}$
1 (wallrock)	+0.52	−7.39
2 (wallrock)	+0.70	−6.65
3 (vein)	−0.16	−10.15
4 (vein)	+0.16	−10.2
5 (vein)	+0.14	−10.37
6 (vein)	+0.16	−9.80
7 (vein)	+0.02	−10.4
8 (vein)	−0.05	−10.03
9 (vein)	−0.16	−10.01
10 (vein)	+0.12	−10.44
11 (vein)	+0.17	−10.04

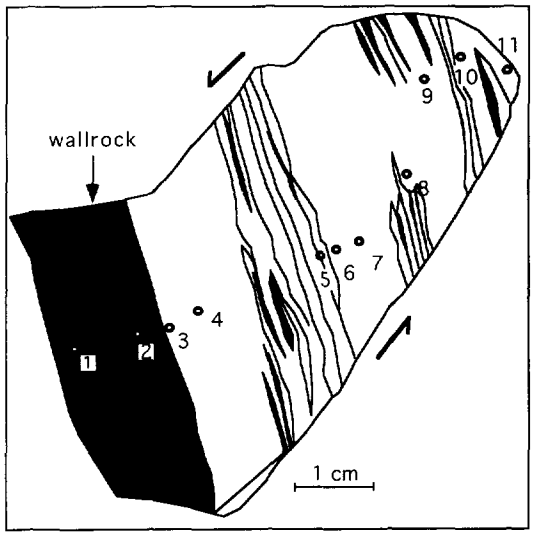

Fig. A1. Location of stable isotope analyses from specimen taken from locality 9 on Fault 2.

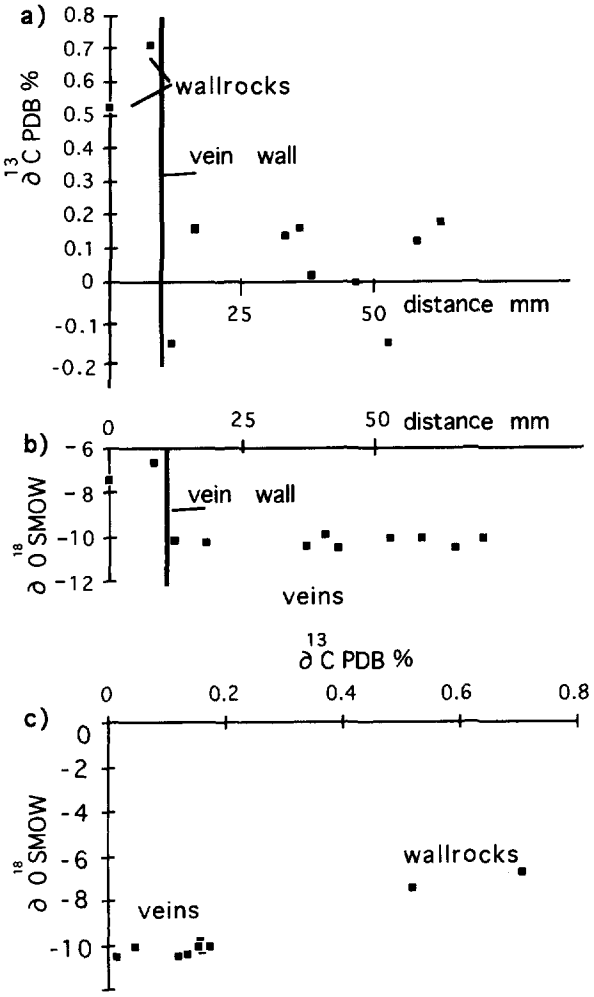

Fig. A2. (a) Plot of $\partial^{13}C_{PDB}$‰ against distance across the pull-apart, with distance measured from the hangingwall, locality 9, Fault 2. The increments of mineralization get older with increasing distance from the wall-rock, and there is no systematic change in isotope composition with inferred age of the increments. (b) Plot of $\partial^{18}O_{SMOW}$ against distance across the pull-apart, with distance measured from the hangingwall. The crack-seal veins do not show a systematic change with inferred age of the increments. (c) Plot of $\partial^{13}C_{PDB}$‰ against $\partial^{18}O_{SMOW}$ for calcite veins and wallrocks at locality 9 on Fault 2.